Food Chemistry: X 24 (2024) 101962

Contents lists available at ScienceDirect

Food Chemistry: X

journal homepage: www.sciencedirect.com/journal/food-chemistry-x

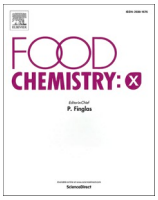

Improve the fiber structure and texture properties of plant-based meat analogues by adjusting the ratio of soy protein isolate (SPI) to wheat gluten (WG)

Lianzhou Jiang [1], Hongyang Zhang [1], Jiayu Zhang, Sibo Liu, Yachao Tian, Tianfu Cheng, Zengwang Guo [*], Zhongjiang Wang [*]

College of Food Science, Northeast Agricultural University, Harbin, Heilongjiang 150030, China

ARTICLE INFO

Keywords:
Soy protein isolate
Wheat gluten
Meat analogues
Texture
Rheology

ABSTRACT

The effects of the ratio change of SPI and WG (11: 1, 10: 2, 9: 3, 8: 4, 7: 5, 6: 6 and 5: 7) on the product characteristics of plant-based meat analogues (PBMAs) were investigated. The results show that the addition of WG significantly reduces the hardness and chewiness of PBMAs, but significantly improves the springiness and brightness of PBMAs. When the ratio of SPI to WG is 9: 3, PBMAs has the best fiber structure, storage modulus and apparent viscosity. Fourier transform infrared spectroscopy (FT-IR) results showed that the transition from α-helix to β-fold was an important reason for PBMAs fibers reinforcement. The intermolecular interaction of protein shows that the enhancement of fiber structure of PBMAs is related to the increase of disulfide bonds. In this study, low cost and high simulation degree PBMAs are provided as a reference for developing PBMAs.

1. Introduction

Plant-based meat analogues (PBMAs) are mainly prepared from plant protein by extrusion, electrostatic spinning and other technologies (Mohamad Mazlan et al., 2020; Xia et al., 2023; Zhang, Yang, et al., 2023). At present, extrusion technology is the most efficient method of preparing PBMAs (He et al., 2020). Based on the moisture content of the final extruded product, extrusion technology mainly includes low moisture extrusion (20–40 % moisture) and high moisture extrusion (40–80 % moisture) (Zhao et al., 2024). High moisture extrusion technology has many processing advantages over low moisture extrusion technology, including a lower energy input and a higher degree of simulation (Prabha et al., 2021; Zhang, Zhao, et al., 2023). Therefore, the production of PBMAs by high moisture extrusion technology will be more in line with the food industry development trend. PBMAs have similar taste, texture, and nutritional value to animal meats (Nakagawa et al., 2024). Compared with the animal meat, PBMAs can save land and water resources, and has a lower carbon footprint (Choudhury et al., 2020). In addition, PBMAs are also able to meet the needs of vegetarian and religious activists (Nam et al., 2024). Furthermore, PBMAs have the potential to provide a more sustainable and environmentally friendly source of protein (Singh et al., 2021). Consequently, the pursuit of novel PBMAs has emerged as a prevalent research focus within the food industry.

Myofibrillar protein (MP) is the main structural component of meat, which plays an important role in maintaining the overall quality, juiciness and flavor of meat during processing and consumption. PBMAs has a fiber structure similar to MP. This structure helps provide the chewiness and mouthfeel that are characteristic of traditional meat. At present, the plant proteins that can produce PBMAs by high-moisture extrusion technology mainly include soybean protein isolate (SPI) (Schreuders et al., 2019; L. Yang et al., 2023), wheat gluten protein (WG) (Sun et al., 2024; Zhang, Yang, et al., 2023), pea protein (Zhu et al., 2021), peanut protein (Zhang, Yang, et al., 2023) etc. Among them, SPI has the advantages of low price, easy access, balanced amino acid composition and high bioavailability (Cofrades et al., 2023; Tian, Sun, et al., 2023), and is gradually becoming the leading raw material for PBMAs (Shaghaghian et al., 2022). In addition, SPI, having served as a high-quality source of protein, had the functions of enhancing immunity and controlling blood sugar. Although the current technology for producing PBMAs is mature, its high production cost has hindered its popularization. To further reduce production costs, we found that some

* Corresponding authors.
E-mail addresses: gzwname@163.com (Z. Guo), wzjname@126.com (Z. Wang).
[1] These authors contributed equally to this work.

https://doi.org/10.1016/j.fochx.2024.101962
Received 7 August 2024; Received in revised form 10 October 2024; Accepted 1 November 2024
Available online 4 November 2024

cheaper defatted soybean powder (DSP) could be added to the production of PBMAs. However, we found that the texture of PBMAs made of SPI and DSP is poor, which cannot meet the requirements of consumers for its fiber structure. Previous studies have found that adding a certain proportion of WG to soybean protein concentrate can improve the texture and fiber characteristics of PBMAs (Chiang et al., 2019). A recent study found that adding WG into pea protein can improve the textural properties and fiber structure of PBMAs (Zhao et al., 2024). The reason is that pea protein and WG, two thermodynamically incompatible components, can prevent the horizontal aggregation of protein and are beneficial to the longitudinal arrangement to form fiber structure (Grabowska et al., 2016; Zhao et al., 2024). This means that WG can be an effective ingredient to improve the textural properties and fiber structure of PBMAs, making them more suitable for food applications. Inspired by this study, we believe that the combination of WG and SPI will be the key point to improve the structure and properties of SPI-WG-DSP PBMAs.

Although the improvement of soy protein-based PBMAs by WG has been reported, the focus is mainly on binary mixed systems. However, there is still a gap in research on improving the texture and fiber structure of PBMAs prepared by SPI-WG-DSP ternary system by adjusting the ratio of SPI to WG. Therefore, in this study, SPI and WG are mixed in different proportions (SPI: WG = 5:7, 6:6, 7:5, 8:4, 9:3, 10:2, 11:1). The addition proportion of DSP is determined according to our pre-experimental results. PBMAs was prepared by high moisture extrusion. The hardness and chewiness of PBMAs were measured by texture analyzer. The changes of fiber structure of PBMAs were observed by scanning electron microscope (SEM). The rheological characterization of PBMAs was carried out to deeply understand the structural formation and physical and chemical changes during extrusion processing. In order to deeply understand the interaction between SPI and WG, the secondary structure, thermodynamic properties and intermolecular interaction force of PBMAs were analyzed. The results of this study can be used to develop more efficient production methods for PBMAs, as well as the optimization of its application in the food industry.

2. Materials and methods

2.1. Materials

SPI、DSP and WG were provided by Yuwang Group (Shandong Province, China). SPI contains around 85.0 % protein, 12.5 % carbohydrate, 1.0 % fat, and 3.0 % moisture. DSP contains around 65.0 % protein, 26.5 % carbohydrate, 0.6 % fat, and 6.5 % moisture. WG contains around 83.5 % protein, 3.5 % moisture, 10.5 % carbohydrate, and 1.5 % fat. Shanghai Yuanye Biotechnology Co., Ltd. (Shanghai, China) and Sinopharm Chemical Reagent Co., Ltd. (Shanghai, China) provided other chemicals and reagents.

2.2. PBMAs preparation

PBMAs were prepared using a modified method based on previous research (Hou et al., 2023). According to Table 1, mix SPI, WG and DSP evenly, with the total dry basis accounting for 50 % (*w*/w) and moisture content accounting for 50 % (w/w). PBMAs was prepared by DS56-III twin-screw extruder (Jinan Saixin Machinery Co., Ltd., China) through high moisture extrusion experiment. The feed rate was set at 12.0 kg/h, the screw speed was adjusted to 300 r/min, and the temperatures of the various modules of the extruder were maintained at 60, 80, 120, 150, and 170 °C respectively. Meanwhile, the cooling zone was kept below 50 °C through the circulation of running water. PBMAs samples were cut into strips with a width of 20 cm and a length of 30 cm. And PBMAs was stored in a refrigerator at −20 °C for subsequent analysis.

Table 1
Formulation of PBMAs.

Samples	Formulations		
	SPI	WG	DSP
SPI:WG = 5:7	5	7	6
SPI:WG = 6:6	6	6	6
SPI:WG = 7:5	7	5	6
SPI:WG = 8:4	8	4	6
SPI:WG = 9:3	9	3	6
SPI:WG = 10:2	10	2	6
SPI:WG = 11:1	11	1	6

2.3. Texture properties

By improving the previous research methods, the detection method for samples textural properties was determined (Hou et al., 2023). PBMAs samples were fixed on the platform, and the textural profile of PBMAs were analyzed by Brookfield CT3 texture analyzer (Brookfield, USA). TPA mode was selected for testing, with probe descending speed of 2 mm/s, testing speed of 0.5 mm/s and rising speed of 2 mm/s, and compressed to 50 % of its original thickness.

2.4. Color measurement

Having improved upon the previous research methods, the detection method for samples of color was determined (Deng et al., 2023). Utilized the NR60CP+ hand-held colorimeter (Shenzhen Sanenshi Technology Co., Ltd., China) to detect the color change of PBMAs, and record the values of L*, a* and b*. Where L* stands for the brightness of color, a* stands for redness and b* stands for yellowness. The measurements were repeated three times and the average values were used to calculate the color change. The values were compared with the initial values to determine the amount of color change. Calculate the total color difference (ΔE) by the following formula:

$$\Delta E = \sqrt{\left(L_{sample} - L_{standard^*}\right)^2 + \left(a_{sample} - a_{standard^*}\right)^2 + \left(b_{sample} - b_{standard^*}\right)^2} \quad (1)$$

2.5. Scanning electron microscopy (SEM)

According to our previous method (Y. Tian et al., 2024), the microstructure of the sample was observed by scanning electron microscope (SEM, Hitachi Manufacturing Co., Ltd., Japan). Micrographs were photographed at magnification levels of × 500, × 1000, and × 1500, respectively.

2.6. Low-field nuclear magnetic resonance (LF-NMR) measurements

The LF-NMR detection of PBMAs was based on previous research methods and was carried out after appropriate modifications had been made (Kang & Ma, 2023). In order to confirm the relaxation measurements of the sample, an LF-NMR analyzer (NMI20-030 V-I, Niumag Inc., China) was used. With 3000 ms waiting time, 0.10 ms echo time, and 6 scans, the Carr-Purcell-Meiboom-Gill (CPMG) sequences were used to investigate spin-spin relaxation time (T2). Measured relaxation times were converted to corresponding relaxation signal components.

2.7. Measurements of rheological properties

The determination method of rheological properties was determined by improving our previous method (Tian et al., 2022). Specifically, the rheometer MCR 101 (Anton Paar, Austria) with parallel plates with a diameter of 50 mm was used to measure the rheology. Before measurement, stress scanning is carried out to determine the linear viscoelastic region. Shear stress, shear rate and apparent viscosity were also measured.

2.8. FT-IR measurements

The FT-IR detection of PBMAs was based on previous research methods and was carried out after appropriate modifications had been made (Tian et al., 2022). To observe the FT-IR spectra of the samples, a Fourier transform infrared spectrometer (PerkinElmer, Shelton, USA) was used. From 400 to 4000 cm^{-1}, the samples were scanned eight times at full speed.

2.9. Thermal properties measurements

The determination method of thermal properties was determined by improving our previous method (Y. Tian et al., 2024). The thermal characteristics of PBMAs were investigated using a different scanning calorimeter (DSC25, TA Instruments, America). In an aluminum crucible, 4 mg of sample was accurately weighed, sealed, and heated from 30 °C at a heating rate of 20 °C per minute to 160 °C.

2.10. Protein intermolecular interaction force measurements

Protein solubility of PBMAs was measured by previous research methods, with minor modifications to evaluate the protein-protein interaction (J. Zhang et al., 2019; Zhao et al., 2024). Initially, prepared the following four solvents: (1) 0.1 mol/L phosphate buffer solution (PBS) at pH 7.4, (2) 8 mol/L urea dissolved in the phosphate buffer solution (designated as PU), (3) 2 % (*v*/v) β-mercaptoethanol (β-Me) added to the phosphate buffer solution (PM), and (4) 1.5 % (*w*/*v*) sodium dodecyl sulfate (SDS) mixed into the phosphate buffer solution (PS).

Next, the PBMAs were subjected to freeze-drying, followed by grinding and sieving through a 100-mesh sieve. This process was repeated to ensure consistency. Then, 100 mg of the PBMAs powder was thoroughly mixed with 10 mL of each of the prepared solvents. After ensuring uniform mixing, the samples were shaken for 12 h. Subsequently, they were centrifuged at 10,000*g* for 15 min. The total protein content in the sample was determined by the Kjeldahl method, and the protein content in the supernatant was determined by the Lowery method. Based on these measurements, the protein solubility was calculated using the following formula:

$$Solubility(\%) = \frac{S_1}{S_0} * 100 \quad (2)$$

where S_0 represents the protein content of the supernatant and S_1 represents the total protein of the original sample. According to the solubility difference of PBMAs in different solvents, various chemical crosslinking bonds are calculated.

2.11. Statistical analysis

All analyses were conducted using IBM SPSS 21.0 (IBM Corporation, USA). A one-way ANOVA was used to compare each dependent variable between groups. To analyze the differences between individual means, Duncan's multiple range test was used ($p < 0.05$). Each experiment was conducted at least three times, and the results were expressed as mean

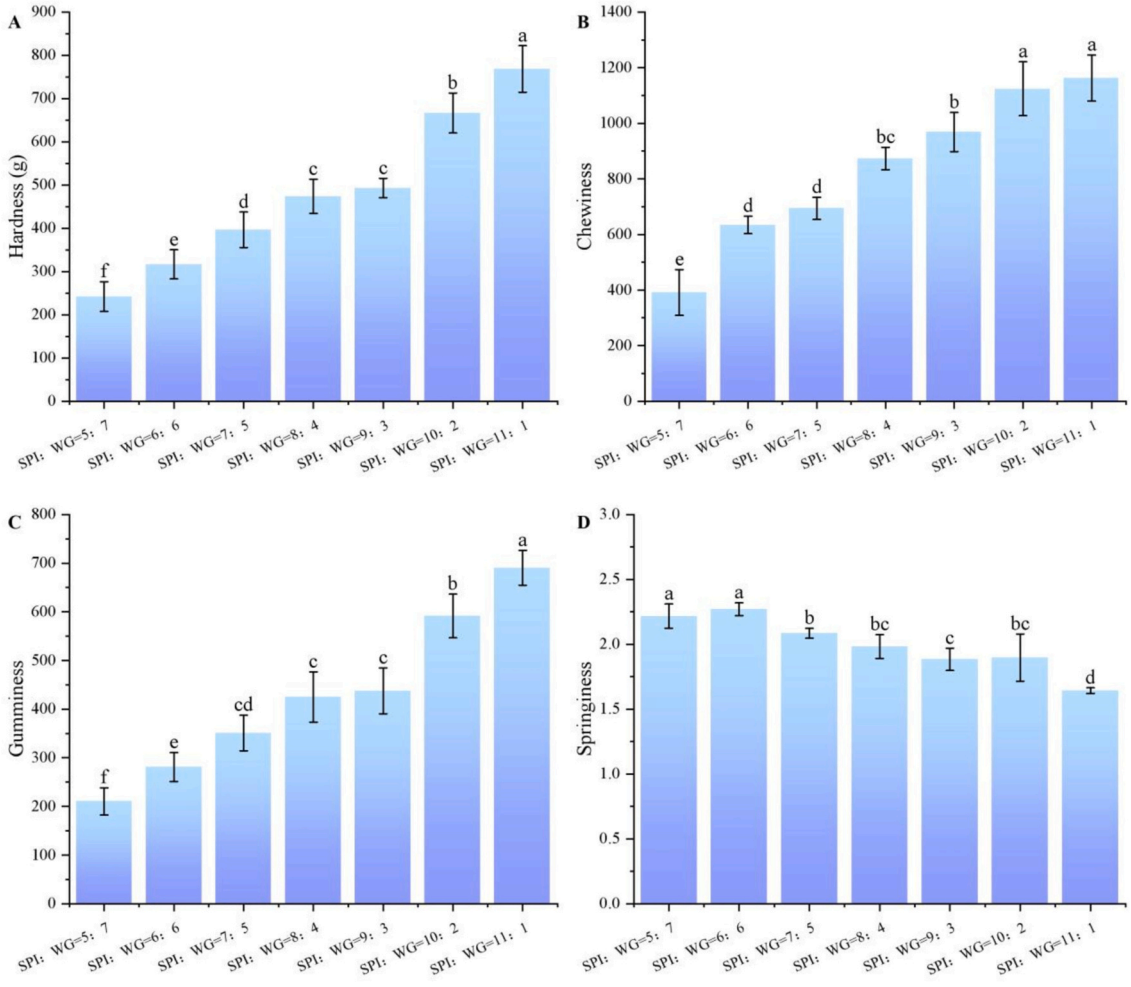

Fig. 1. Effect of the SPI to WG ratio on the texture properties of the PBMAs. Different letters indicate significant differences ($p < 0.05$).

± standard deviation.

3. Results and discussion

3.1. Texture properties analysis

Textural analysis measures the physical properties of the meat analogue, such as the hardness, gumminess, chewiness, and springiness, which are important indicators of its quality (Chen et al., 2022). The effect of the SPI and WG ratio on the texture properties of PBMAs was shown in Fig. 1. In Fig. 1 (A), (B), and (C), it was demonstrated that there was a linear increase in the hardness, chewiness, and gumminess of the PBMAs sample as the SPI ratio was progressively augmented. This shows that adding SPI will make PBMAs harder. At the same time, the springiness of PBMAs decreased with the increase of SPI ratio. When the SPI ratio was high (SPI: WG = 10:2 and 11:1), it was observed that there was insufficient WG to serve as the skeletal structure within PBMAs, leading to inadequate fiber bonding. This finding was similar to previous studies (Hou et al., 2023; Zhang et al., 2022). However, it was found that excessive SPI led to overly high hardness and chewiness in the extruded PBMAs. This, in turn, diminished the taste experience of the PBMAs and ultimately had a negative impact on the overall taste of the products. When the ratio of SPI to WG was 7:5, 6:6, and 5:7, it was observed that the PBMAs exhibited excessively low levels of hardness, chewiness, and gumminess. The PBMAs with inadequate hardness lacked sufficient chewing sensation, thereby impacting the eating experience negatively. Moreover, these foods with low hardness were often more prone to external factors such as extrusion and deformation, which had increased the difficulty and cost involved in the processes of storage and transportation. When the ratio of SPI to WG was set at 9:3 and 8:4, it was observed that the PBMAs demonstrated moderate levels of hardness, chewiness, and gumminess. This moderate texture proved advantageous for the further development and utilization of these products. This moderate texture was preferred by consumers because it provided a pleasant balance between hardness and chewiness.

3.2. Color analysis

Color plays an important role in PBMAs products, and it also affects consumers' acceptance of them (He et al., 2020). The color parameters of PBMAs, which had different SPI and WG ratios, were presented in Table 2. From Table 2, it was evident that with the increase in WG content, the L* and b* values of PBMAs generally exhibited an increasing trend. Specifically, when the ratio of SPI to WG was 11:1, the minimum L* value was recorded as 41.60 ± 0.82, whereas at a ratio of 5:7, the maximum L* value reached 66.21 ± 1.13. This observation indicated that WG enhanced the brightness of PBMAs (Tian, Ren, et al., 2023). Furthermore, as the WG content increased, the values of a* and ΔE decreased notably. At an SPI to WG ratio of 11:1, the maximum ΔE value was found to be 16.31 ± 0.82. However, with a greater proportion of WG, the ΔE value generally followed a downward trend, suggesting that incorporating more WG led to lighter-colored extrudates. Previous studies had found that the Maillard reaction was the main factor affecting the color of meat analogues, which formed protein-sugar adducts and highly colored insoluble polymers called melanoids during extrusion cooking (Zhang, Zhao, et al., 2023). In this study, a higher proportion of WG significantly increased the whiteness of PBMAs, which may have been due to the lower sugar content of WG compared with SPI. This discovery is similar to the previous research results (Zhao et al., 2024). Generally, consumers' acceptance of PBMAs with darker colors is low (Zhao et al., 2024). Consequently, it was more advantageous for product promotion to improve the whiteness of PBMAs by incorporating an appropriate proportion of WG.

Table 2
Effect of SPI and WG compound ratio on PBMAs color value.

Samples	L*	a*	b*	ΔE
SPI:WG = 5:7	66.21 ± 1.13^{a}	7.56 ± 0.88^{c}	26.21 ± 0.51^{a}	11.19 ± 0.80^{c}
SPI:WG = 6:6	47.44 ± 0.46^{b}	11.29 ± 0.08^{ab}	22.70 ± 0.29^{b}	10.77 ± 0.37^{c}
SPI:WG = 7:5	44.32 ± 1.44^{c}	12.11 ± 0.39^{a}	22.31 ± 1.29^{bc}	13.82 ± 1.21^{b}
SPI:WG = 8:4	45.74 ± 0.48^{bc}	11.63 ± 0.26^{a}	20.83 ± 0.62^{cd}	12.06 ± 0.37^{bc}
SPI:WG = 9:3	46.66 ± 0.42^{bc}	10.57 ± 0.23^{b}	20.43 ± 1.01^{cd}	11.20 ± 0.43^{c}
SPI:WG = 10:2	45.00 ± 2.64^{c}	11.40 ± 0.68^{ab}	20.83 ± 1.16^{d}	12.93 ± 2.55^{bc}
SPI:WG = 11:1	41.60 ± 0.82^{d}	12.08 ± 0.30^{a}	18.50 ± 0.25^{e}	16.31 ± 0.82^{a}

Note: Results are expressed as mean value ± standard deviation. Different lowercase letter in the same column means significant differences ($p < 0.05$).

3.3. Microstructure analysis

Microstructure observation played a pivotal role in the past studies of meat analogues, aiding researchers in understanding their composition and distinct characteristics (Dekkers et al., 2018). Fig. 2 shows the effect of SPI to WG ratio on the microstructure of PBMAs. As Fig. 2 shows, when the ratio of soy protein isolate (SPI) to wheat gluten (WG) was 11:1 or 10:2, cracks were observed on the surface of the PBMAs, and no distinct fibrous structure was apparent. When the ratio of SPI to WG was 9:3, the surface of the PBMAs exhibited a prominent fibrous structure aligned along the extrusion direction, and this distribution was uniform and orderly. However, as the proportion of WG increased, the fiber structure of the PBMAs became thicker, and the degree of orderliness decreased. Ultimately, when the ratio of SPI to WG reached 6:6 or 5:7, no discernible fibrous structure was observed on the surface of the PBMAs. This phenomenon could be attributed to the optimal ratio of SPI to WG being 9:3, which effectively prevented protein aggregation and facilitated protein rearrangement to form a fibrous structure (Hou et al., 2023). Nevertheless, an excessive amount of WG (SPI:WG ratios of 6:6 and 5:7) interfered with protein recombination, thereby compromising the fiber structure of the PBMAs. This finding resonates with the observations made by Zhao et al. (Zhao et al., 2024), who posited that excessive WG led to a viscous extrudate characterized by a markedly weaker chewy texture, impeding the alignment of protein fibers along the extrusion direction. In summary, the most favorable SPI to WG ratio was found to be 9:3, resulting in PBMAs that displayed a pronounced fibrous structure. Fiber structure and texture are the most important properties of PBMAs. In this study, the ratio of SPI to WG is 9:3, which is the best ratio for preparing PBMAs. A small amount of WG (SPI: WG = 11:1 and 10:2) has no significant effect on improving the fibrous structure of PBMAs, while excessive WG (SPI: WG = 6:6 and 5:7) hinders fiber formation.

3.4. Water distribution analysis

LF-NMR is an important index to characterize the distribution and migration of water in meat analogs (Kaysen et al., 2022). As a measure of water molecules' mobility, T_2 is the time needed to excite a spin-spin proton to exchange energy with adjacent protons (Hou et al., 2023; Qin et al., 2022). As shown in Fig. 3, the effect of the SPI to WG ratio on the T2 relaxation time distribution curve of the PBMAs. With the increase in degrees of freedom, the peak states can be divided into T_{2b} and T_{21} (bound water), T_{22} (immobilized water) and T_{23} (free water). Table 3 shows the proportion of T2 distributions. With the ratio of SPI to WG changing from 11: 1 to 5: 7, the proportion of P_{21} increased from 8.02 ± 0.35 to 16.13 ± 0.43. This indicated that, as the content of WG increased, the binding capacity of the PBMAs samples to water molecules also rose (Hou et al., 2023). In addition, P_{22} accounted for the highest proportion, and with the increase of WG content, the proportion

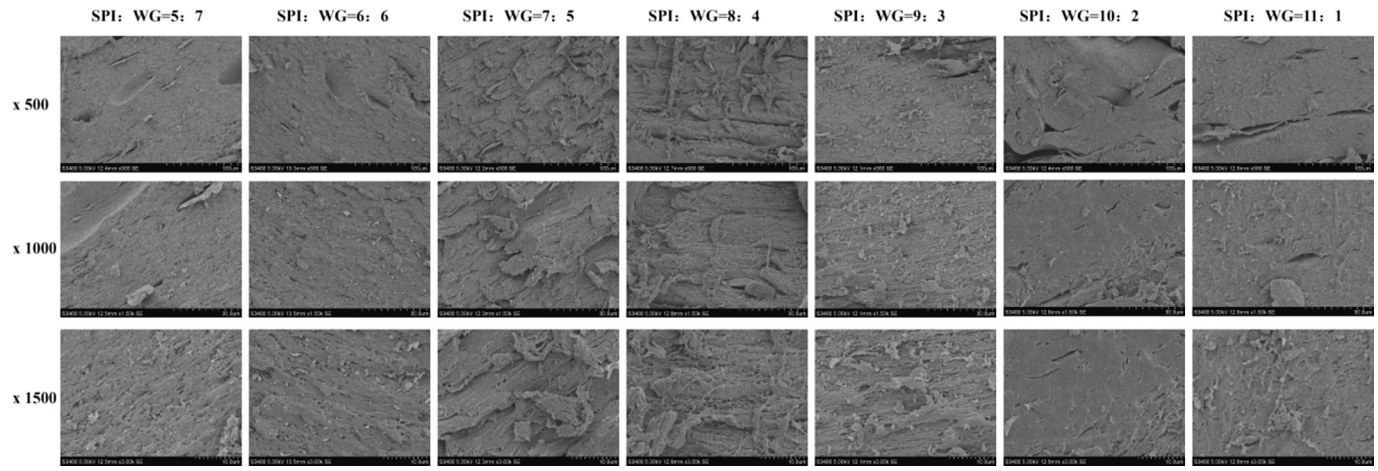

Fig. 2. Effect of the SPI to WG ratio on the microstructure of the PBMAs.

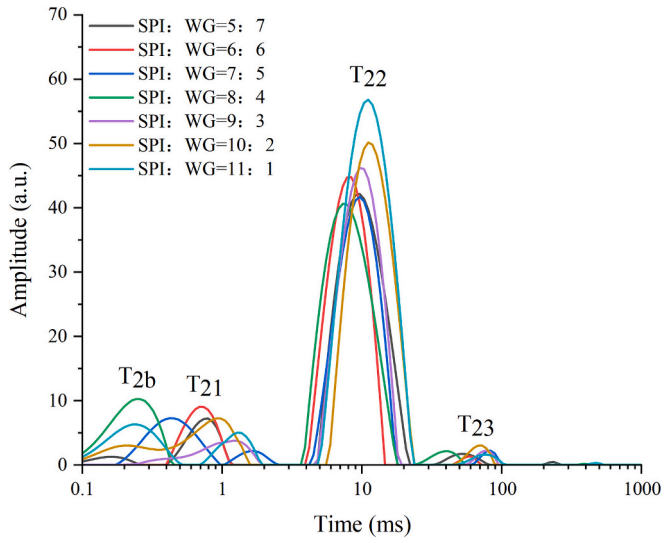

Fig. 3. Effect of the SPI to WG ratio on the T2 relaxation time distribution curve of the PBMAs.

Table 3
Effect of the SPI and WG compound ratio on the T2 relaxation time of the PBMAs.

Samples	P_{21}(%)	P_{22}(%)	P_{23}(%)
SPI:WG = 5:7	16.13 ± 0.43^{a}	82.40 ± 0.23^{e}	1.47 ± 0.35^{a}
SPI:WG = 6:6	16.10 ± 0.51^{a}	82.43 ± 0.18^{e}	1.45 ± 0.29^{a}
SPI:WG = 7:5	14.47 ± 0.30^{b}	84.06 ± 0.39^{d}	1.47 ± 0.42^{a}
SPI:WG = 8:4	13.51 ± 0.48^{c}	85.27 ± 0.57^{c}	1.22 ± 0.22^{ab}
SPI:WG = 9:3	12.73 ± 0.42^{d}	86.00 ± 0.65^{c}	1.26 ± 0.21^{ab}
SPI:WG = 10:2	9.84 ± 0.71^{e}	89.25 ± 0.61^{b}	0.91 ± 0.16^{bc}
SPI:WG = 11:1	8.02 ± 0.35^{f}	91.25 ± 1.16^{a}	0.73 ± 0.11^{c}

Note: Results are expressed as mean value ± standard deviation. Different lowercase letter in the same column means significant differences ($p < 0.05$).

of P_{22} decreased from 91.25 ± 1.16 to 82.40 ± 0.23. Accordingly, P_{22} is the main form of water molecules in PBMAs, and WG can promote the transformation of bound water into immobilized water and free water (Hou et al., 2023). With the increase of the proportion of WG, the proportion of P_{23} increased from 0.73 ± 0.11 to 1.47 ± 0.35. Generally speaking, the different proportions of SPI and WG will affect the water distribution of PBMAs (Guo et al., 2020). Understanding the T2 distributions in PBMAs is crucial for optimizing their texture and hydration properties. By analyzing the different forms of water within the samples, researchers can tailor the SPI to WG ratios to achieve desired moisture levels and stability. This information is vital for improving the quality and consumer acceptance of meat analogues.

3.5. Rheological properties analysis

Rheological properties can be used to describe the fluidity and viscosity of meat analogues under different conditions, and can also reflect the interaction mechanism between different components (Tian et al., 2024). The storage modulus (G') and loss modulus (G") of PBMAs with different SPI and WG ratios are shown in Fig. 4(A) and (B). With the increase of vibration frequency, both G' and G" increase, and the value of G' is much higher than G", which indicates that the elasticity of samples is dominant (Tian et al., 2022). This also indicates that in the linear viscoelastic range, the change of frequency will not destroy the structure of PBMAs (Hou et al., 2023). When the ratio of SPI to WG changed from 11: 1 to 9: 3, with the increase of WG content, G' and G" increased, and the ratio of WG continued to increase, and G' and G" began to decline. This shows that the interaction between SPI and WG in a proper proportion (SPI: WG = 9:3) can strengthen the fiber structure of PBMAs, while excessive WG (SPI: WG = 6:6 and 5:7) will hinder the formation of fiber structure. This phenomenon can be explained by SEM in Fig. 2.

Fig. 4(C) shows the apparent viscosity change of PBMAs. The viscosity of PBMAs decreases with the increase of shear rate, which indicates that PBMAs has shear thinning characteristics (Hou et al., 2023). It was linked to protein interactions destruction during shearing (Zhao et al., 2024). The shearing process disrupted the interactions between proteins, preventing them from forming the fiber structures. This led to a decrease in the protein's stability. When the ratio of SPI to WG is 9: 3, the viscosity of PBMAs is the highest, which shows that the molecular interaction between SPI and WG is the strongest under this ratio. Generally, the increase of viscosity is usually beneficial to the formation of fibrous structure, because high viscosity causes the pressure of extruder to increase, so that protein network structure can be extended to form fibrous structure (Hou et al., 2023). PBMAs that possessed high viscosity had the potential to be highly advantageous in the food industry, particularly for the creation of meat analogs and plant-based protein products, as their fibrous structure closely replicated that of animal meat. Furthermore, these PBMAs might find applications in the development of specialized dietary products for individuals requiring high-protein intake (Del Bo' et al., 2024).

3.6. FT-IR analysis

Studies have confirmed that FT-IR is a method to measure the

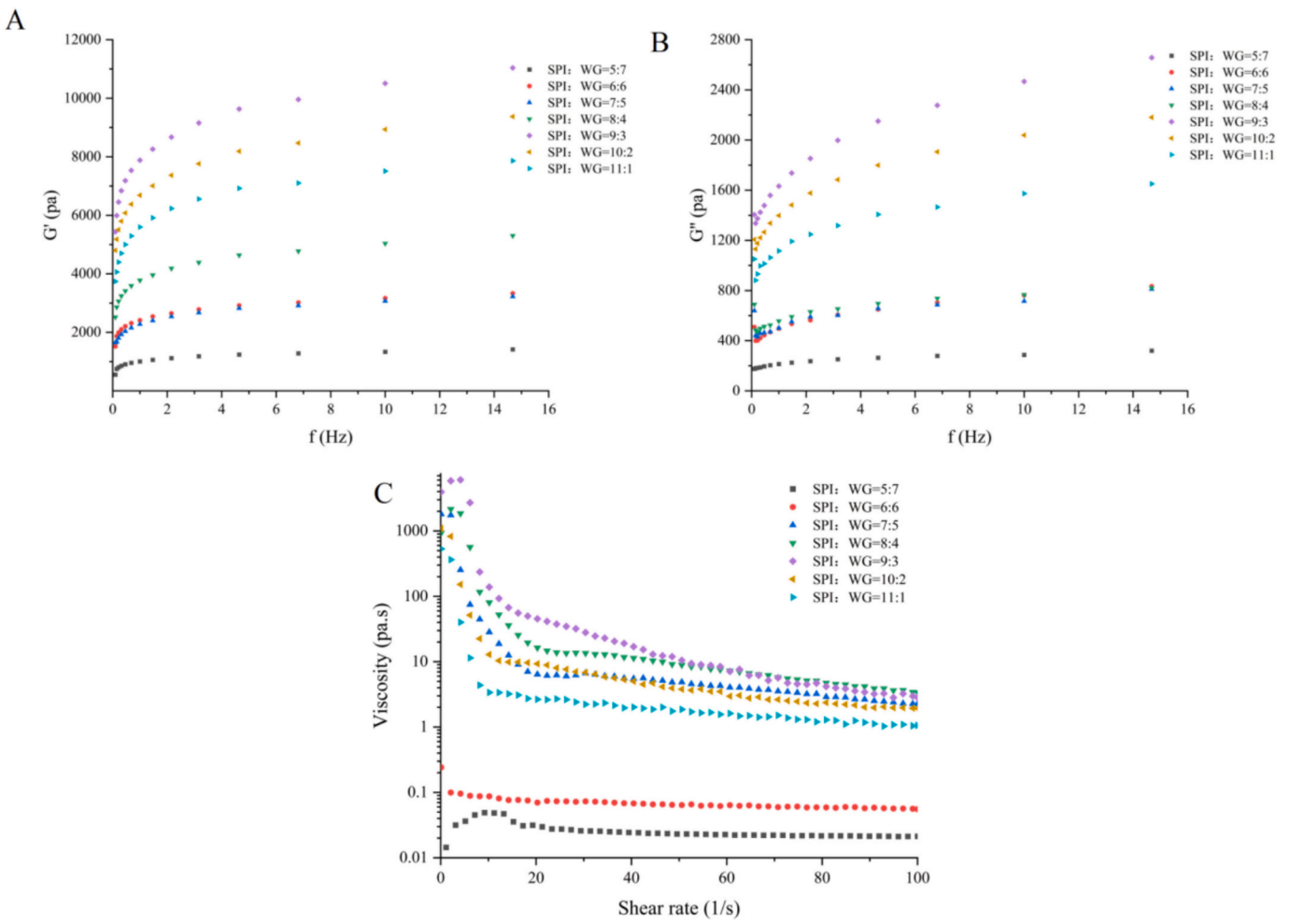

Fig. 4. Effect of the SPI to WG ratio on the rheological properties of PBMAs. A is the G' diagrams of the PBMAs; B is the G" diagrams of the PBMAs; C is the viscosity diagrams of the PBMAs.

vibration state of protein chemical bonds, which can be used to study the secondary structure of proteins (S. Yang et al., 2022). The secondary structure information of protein is mainly in the amide I band (1700–1600 cm^{-1}) of FT-IR spectrum. In this study, the secondary structure of protein was obtained by deconvolution of amide I band by second derivative fitting, and the proportion of protein secondary structure was expressed by the percentage of each designated peak area to the total area of amide I band. FT-IR spectra of PBMAs with different SPI and WG ratios are shown in Fig. 5, and the contents of different secondary structures are shown in Table 4. It can be seen from Table 4 that when the ratio of SPI to WG changes from 11: 1 to 9: 3, the α-helix content decreases from 24.53 ± 0.76 to 16.63 ± 1.65, and the β-sheet

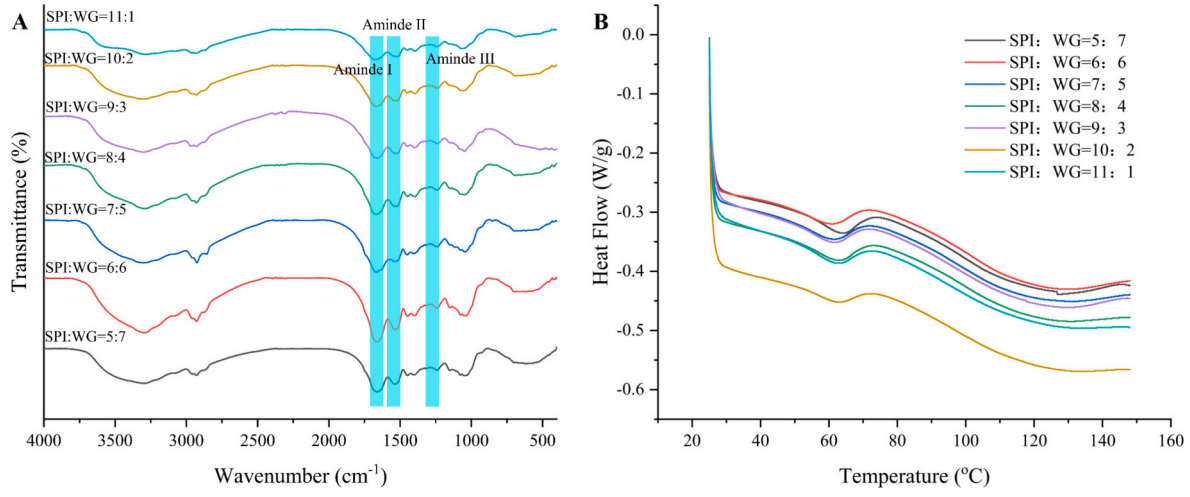

Fig. 5. Effect of the SPI to WG ratio on the FTIR (A), DSC thermogram (B), and the intermolecular force of the PBMAs.

Table 4
Effect of SPI and WG compound ratio on the secondary structures of PBMAs.

Samples	α-helix (%)	β-sheet (%)	β-turn (%)	Random coil (%)
SPI:WG = 5:7	34.47 ± 0.79^{a}	34.68 ± 0.38^{d}	15.37 ± 0.50^{c}	15.48 ± 0.95^{e}
SPI:WG = 6:6	31.09 ± 1.18^{b}	36.64 ± 0.66^{c}	16.3 ± 0.98^{c}	15.97 ± 0.75^{de}
SPI:WG = 7:5	27.08 ± 0.54^{c}	36.78 ± 0.73^{c}	18.82 ± 0.30^{b}	17.32 ± 0.82^{cd}
SPI:WG = 8:4	23.08 ± 0.82^{d}	37.95 ± 0.60^{b}	19.65 ± 0.54^{b}	19.32 ± 1.09^{ab}
SPI:WG = 9:3	16.63 ± 1.65^{f}	42.08 ± 0.53^{a}	21.27 ± 0.79^{a}	19.82 ± 0.37^{a}
SPI:WG = 10:2	20.50 ± 0.85^{e}	38.47 ± 0.54^{b}	22.06 ± 1.30^{a}	18.97 ± 1.20^{abc}
SPI:WG = 11:1	24.53 ± 0.76^{d}	38.33 ± 0.96^{b}	19.21 ± 0.94^{b}	17.93 ± 0.97^{bc}

Note: Results are expressed as mean value ± standard deviation. Different lowercase letter in the same column means significant differences ($p < 0.05$).

content increases from 38.33 ± 0.96 to 42.08 ± 0.53. This shows that increasing the proportion of WG properly can promote the transformation from α-helix to β-sheet, which is beneficial to protein aggregation and fiber structure formation (Hou et al., 2023; Zhao et al., 2024). When the ratio of SPI to WG changed from 9: 3 to 5: 7, with the increase of WG ratio, the α-helix content increased from 16.63 ± 1.65 to 34.47 ± 0.79, and the β-sheet content decreased from 42.08 ± 0.53 to 38.33 ± 0.96. This shows that excessive WG is not conducive to enhancing the stability and fiber structure of PBMAs (Zhao et al., 2024). In summary, a moderate increase in WG content promotes the transformation from α-helix to β-sheet, which is beneficial for protein aggregation and fiber structure formation. However, when the WG content becomes excessive, it leads to a further decrease in β-sheet content and an increase in α-helix content, ultimately destabilizing the PBMA structure. Therefore, it is crucial to balance the WG ratio to optimize the structural integrity and functionality of PBMAs.

3.7. Thermal properties analysis

DSC can be used to detect the thermal stability of meat analogues, and then to judge the structural and protein conformational changes (Hou et al., 2023). The influence of SPI and WG in different proportions on the thermal stability of PBMAs shown in Fig. 5 (B). As can be seen from the Figure, an obvious bimodal phenomenon is observed in the DSC curve of PBMAs. This shows that SPI, WG and DSP have interactions, which may lead to the thermal behavior of DSC curve different from that of single substance. In addition, the appearance of double peaks may also be related to the fact that PBMAs contains a certain proportion of DSP. The composition of DSP is complex and its molecular weight is widely distributed, which may lead to multiple peaks in DSC curve. When the ratio of SPI to WG changes from 11: 1 to 9: 3, with the increase of WG content, the thermal denaturation temperature of PBMAs decreases from 126.96 °C to 123.05 °C, which indicates that the energy required for hydrogen bond breaking between PBMAs molecules decreases during heating (Singh et al., 2021; J. Zhang et al., 2017). When the ratio of SPI to WG changes from 9:3 to 5:7, with the increase in WG content, the thermal denaturation temperature of PBMAs increases. This may be due to the more intense chemical bonding caused by excessive WG, which also leads to unclear fiber structure. The results show that the change of SPI and WG ratio will affect the thermal stability of PBMAs. This finding suggests that adjusting the SPI and WG ratios can be used to fine-tune the thermal properties of PBMAs for specific applications.

3.8. Protein intermolecular interaction force analysis

By analyzing the solubility difference of protein in different reagents, the interaction between protein molecules can be analyzed (Zhao et al., 2024). The principle is that four different reagents can break different types of intermolecular chemical bonds to dissolve protein, thus determining the importance of each specific chemical bond (Tian, Ren, et al., 2023; Zhao et al., 2024). The results of the interaction force of PBMAs are shown in Table 5. It can be seen from Table 5 that disulfide bonds between protein molecules are dominant, followed by ionic bonds and hydrogen bonds, and the content of hydrophobic bonds is the lowest in all PBMAs samples. When the ratio of SPI to WG changes from 11: 1 to 5: 7, with the increase of WG content, the role of hydrogen bonding is gradually enhanced. Hydrogen bond is the main force to keep bound water and fixed water (Lv et al., 2023). This phenomenon shows that the addition of WG can effectively enhance the binding ability of PBMAs with water. With the increase of WG content, the hydrophobic bond content decreases, which may be because SPI has stronger hydrophobic effect than WG (Zhao et al., 2024). With the increase of WG content, the disulfide bond first increases and then decreases. When the ratio of SPI to WG is 9: 3, the disulfide bond content is the highest, which is 86.12 ± 0.17. A disulfide bond is an important chemical bond between protein molecules. Its formation contributes to the interaction between protein molecules, thus promoting the formation of fiber structures. In the preparation process of PBMAs, with the increase of intermolecular disulfide bonds in protein, protein molecules are easier to connect with each other and form a continuous fiber network. Previous studies have also found that the content of disulfide bonds in extrudates can reach the highest level by adding appropriate proportion of WG (Zhang et al., 2022). From the microstructure of the sample (Fig. 2), when the ratio of SPI to WG is 9: 3, PBMAs have the best fiber structure, which indicates that fiber structure formation is related to disulfide bonds (Zhao et al., 2024). Previous studies have reported that disulfide bonds play a very important role in maintaining the structural integrity of meat analogues and forming fibrous structures (Liu & Hsieh, 2008). The presence of disulfide bonds significantly influences the texture of PBMAs by contributing to the formation of a fibrous structure. This fibrous structure is essential for mimicking the texture of meat analogues, providing the characteristic chewiness and mouthfeel. Therefore, optimizing the ratio of SPI to WG to enhance disulfide bond formation can improve the textural quality of PBMAs.

4. Conclusion

In summary, this work successfully proves that the fiber structure and texture properties of PBMAs can be improved by adjusting the ratio of SPI to WG. Upon investigation, it was discovered that a 9:3 ratio of SPI to WG yielded PBMAs with an optimal fiber structure, exhibiting a well-

Table 5
Effect of SPI and WG compound ratio on the protein intermolecular interaction force of PBMAs.

Samples	Ionic bond/%	Hydrogen bond/%	Disulfide bond/%	Hydrophobic bond/%
SPI:WG = 5:7	6.34 ± 0.09^{b}	6.97 ± 0.08^{a}	85.18 ± 0.27^{bc}	1.51 ± 0.05^{c}
SPI:WG = 6:6	6.27 ± 0.18^{b}	6.74 ± 0.06^{b}	85.48 ± 0.28^{b}	1.51 ± 0.07^{c}
SPI:WG = 7:5	6.36 ± 0.05^{b}	6.38 ± 0.07^{c}	85.59 ± 0.30^{b}	1.68 ± 0.02^{bc}
SPI:WG = 8:4	6.32 ± 0.12^{b}	6.32 ± 0.11^{cd}	85.59 ± 0.24^{b}	1.76 ± 0.09^{bc}
SPI:WG = 9:3	5.72 ± 0.06^{d}	6.31 ± 0.13^{cd}	86.12 ± 0.17^{a}	1.85 ± 0.17^{b}
SPI:WG = 10:2	6.08 ± 0.08^{c}	6.20 ± 0.05^{d}	85.79 ± 0.30^{ab}	1.93 ± 0.20^{ab}
SPI:WG = 11:1	7.05 ± 0.11^{a}	6.19 ± 0.09^{d}	84.65 ± 0.19^{c}	2.10 ± 0.17^{a}

Note: Results are expressed as mean value ± standard deviation. Different lowercase letter in the same column means significant differences ($p < 0.05$).

balanced combination of chroma, hardness, chewiness, and elasticity. Furthermore, rheological analysis revealed a correlation between the improved viscosity of PBMAs and the reinforcement of their fiber structure. FT-IR spectroscopy findings indicated that an appropriate blend of SPI and WG facilitates the transition of protein secondary structure from α-helix to β-sheet, thereby enhancing both the fiber architecture and protein stability of PBMAs. Notably, our study also confirmed that the primary intermolecular force contributing to the structure of PBMAs is disulfide bonds, and the strengthening of the fiber structure is intimately tied to an increase in these bonds. The results show that when the ratio of SPI to WG is 9: 3, the prepared PBMAs has the best fiber structure and moderate texture. In the future, PBMAs with excellent texture and fiber can gradually replace animal meat, providing consumers with healthy and convenient choices.

Funding

This research was funded by the "HeiLongjiang Natural Science Fund" Provincial Key R&D Plan (YQ2022C021).

CRediT authorship contribution statement

Lianzhou Jiang: Writing – original draft, Data curation, Conceptualization. **Hongyang Zhang:** Writing – original draft, Visualization, Software. **Jiayu Zhang:** Validation, Investigation. **Sibo Liu:** Methodology, Data curation. **Yachao Tian:** Software, Methodology. **Tianfu Cheng:** Formal analysis, Conceptualization. **Zengwang Guo:** Resources, Funding acquisition, Formal analysis. **Zhongjiang Wang:** Supervision, Investigation, Data curation.

Declaration of competing interest

The authors declare that they have no known competing financial interests or personal relationships that could have appeared to influence the work reported in this paper.

Data availability

Data will be made available on request.

References

Chen, Y. P., Feng, X., Blank, I., & Liu, Y. (2022). Strategies to improve meat-like properties of meat analogs meeting consumers' expectations. *Biomaterials, 287*, Article 121648.

Chiang, J. H., Loveday, S. M., Hardacre, A. K., & Parker, M. E. (2019). Effects of soy protein to wheat gluten ratio on the physicochemical properties of extruded meat analogues. *Food Structure, 19*, Article 100102.

Choudhury, D., Singh, S., Seah, J. S. H., Yeo, D. C. L., & Tan, L. P. (2020). Commercialization of plant-based meat alternatives. *Trends in Plant Science, 25*(11), 1055–1058.

Cofrades, S., Garcimartín, A., Pérez-Mateos, M., Saiz, A., Redondo-Castillejo, R., Bocanegra, A., Benedí, J., & Dolores Álvarez, M. (2023). Stabilized soy protein emulsion enriched with silicon and containing or not methylcellulose as novel technological alternatives to reduce animal fat digestion. *Food Research International, 170*, Article 112833.

Dekkers, B. L., Boom, R. M., & van der Goot, A. J. (2018). Structuring processes for meat analogues. *Trends in Food Science & Technology, 81*, 25–36.

Del Bo', C., Chehade, L., Tucci, M., Canclini, F., Riso, P., & Martini, D. (2024). Impact of substituting meats with plant-based analogues on health-related markers: A systematic review of human intervention studies. *Nutrients, 16*(15), 2498.

Deng, Q., Wang, Z., Fu, L., He, Z., Zeng, M., Qin, F., & Chen, J. (2023). High-moisture extrusion of soy protein: Effects of insoluble dietary fiber on anisotropic extrudates. *Food Hydrocolloids, 141*, Article 108688.

Grabowska, K. J., Zhu, S., Dekkers, B. L., de Ruijter, N. C., Gieteling, J., & van der Goot, A. J. (2016). Shear-induced structuring as a tool to make anisotropic materials using soy protein concentrate. *Journal of Food Engineering, 188*, 77–86.

Guo, Z., Teng, F., Huang, Z., Lv, B., Lv, X., Babich, O., Yu, W., Li, Y., Wang, Z., & Jiang, L. (2020). Effects of material characteristics on the structural characteristics and flavor substances retention of meat analogs. *Food Hydrocolloids, 105*, Article 105752.

He, J., Evans, N. M., Liu, H., & Shao, S. (2020). A review of research on plant-based meat alternatives: Driving forces, history, manufacturing, and consumer attitudes. *Comprehensive Reviews in Food Science and Food Safety, 19*(5), 2639–2656.

Hou, Y., Xia, S., Ma, C., Xue, C., & Jiang, X. (2023). Effects of the soy protein to wheat gluten ratio on the physicochemical and structural properties of Alaska Pollock surimi-based meat analogs by high moisture extrusion. *Food Research International, 173*, Article 113469.

Kang, Z.-L., Xie, J.-J., Li, Y.-P., Song, W.-J., & Ma, H.-J. (2023). Effects of pre-emulsified safflower oil with magnetic field modified soy 11S globulin on the gel, rheological, and sensory properties of reduced-animal fat pork batter. *Meat Science, 198*, Article 109087.

Kaysen, C., Jakobsen, L. M. A., Martin, A., & Bertram, H. C. S. (2022). *Low-field NMR relaxation studies of prototype burgers made from plant-based meat alternatives*.

Liu, K., & Hsieh, F.-H. (2008). Protein–protein interactions during high-moisture extrusion for fibrous meat analogues and comparison of protein solubility methods using different solvent systems. *Journal of Agricultural and Food Chemistry, 56*(8), 2681–2687.

Lv, Y., Xu, L., Tang, T., Li, J., Gu, L., Chang, C., Zhang, M., Yang, Y., & Su, Y. (2023). Gel properties of soy protein isolate-potato protein-egg white composite gel: Study on rheological properties, microstructure, and digestibility. *Food Hydrocolloids, 135*, Article 108223.

Mohamad Mazlan, M., Talib, R. A., Chin, N. L., Shukri, R., Taip, F. S., Mohd Nor, M. Z., & Abdullah, N. (2020). Physical and microstructure properties of oyster mushroom-soy protein meat analog via single-screw extrusion. *Foods, 9*(8), 1023.

Nakagawa, K., Chantanuson, R., Boonarsa, P., Seephua, N., & Siriamornpun, S. (2024). Meat analogue preparation from cricket and rice powder mixtures with controlled textural and nutritional quality by freeze alignment technique. *Food Chemistry: X, 22*, Article 101402.

Nam, J.-K., Lee, J. Y., & Jang, H. W. (2024). Quality characteristics and volatile compounds of plant-based patties supplemented with biji powder. *Food Chemistry: X, 23*, Article 101576.

Prabha, K., Ghosh, P., Abdullah, S., Joseph, R. M., Krishnan, R., Rana, S. S., & Pradhan, R. C. (2021). Recent development, challenges, and prospects of extrusion technology. *Future Foods, 3*, Article 100019.

Qin, L., Fu, Y., Yang, F., Chang, Z., Zou, C., Gao, H., Jiang, D., & Jia, C. (2022). Effects of polysaccharides autoclave extracted from Flammulina velutipes mycelium on freeze-thaw stability of surimi gels. *Lwt, 169*, Article 113941.

Schreuders, F. K., Dekkers, B. L., Bodnár, I., Erni, P., Boom, R. M., & van der Goot, A. J. (2019). Comparing structuring potential of pea and soy protein with gluten for meat analogue preparation. *Journal of Food Engineering, 261*, 32–39.

Shaghaghian, S., McClements, D. J., Khalesi, M., Garcia-Vaquero, M., & Mirzapour-Kouhdasht, A. (2022). Digestibility and bioavailability of plant-based proteins intended for use in meat analogues: A review. *Trends in Food Science & Technology, 129*, 646–656.

Singh, M., Trivedi, N., Enamala, M. K., Kuppam, C., Parikh, P., Nikolova, M. P., & Chavali, M. (2021). Plant-based meat analogue (PBMA) as a sustainable food: A concise review. *European Food Research and Technology, 247*, 2499–2526.

Sun, Y., Dong, M., Bai, J., Liu, X., Yang, X., & Duan, X. (2024). Preparation and properties of high-soluble wheat gluten protein-based meat analogues. *Journal of the Science of Food and Agriculture, 104*(1), 42–50.

Tian, T., Ren, K., Cao, X., Peng, X., Zheng, L., Dai, S., Tong, X., Zeng, Q., Qiu, S., & Wang, H. (2023). High moisture extrusion of soybean-wheat co-precipitation protein: Mechanism of fibrosis based on different extrusion energy regulation. *Food Hydrocolloids, 144*, Article 108950.

Tian, Y., Liu, C., Cheng, J., Li, J., Wang, Z., Yuan, C., & Zhou, L. (2024). Development of soy protein isolate-based orally disintegrating film: Improvement of disintegration speed, mechanical properties, and thermal stability by β-Cyclodextrin. *Lwt, 198*, Article 116037.

Tian, Y., Sun, F., Wang, Z., Yuan, C., Wang, Z., Guo, Z., & Zhou, L. (2023). Research progress on plant-based protein Pickering particles: Stabilization mechanisms, preparation methods, and application prospects in the food industry. *Food Chemistry, X, 101066*.

Tian, Y., Yuan, C., Cui, B., Lu, L., Zhao, M., Liu, P., Wu, Z., & Li, J. (2022). Pickering emulsions stabilized by β-cyclodextrin and cinnamaldehyde essential oil/β-cyclodextrin composite: A comparison study. *Food Chemistry, 377*, Article 131995.

Xia, S., Shen, S., Song, J., Li, K., Qin, X., Jiang, X., Xue, C., & Xue, Y. (2023). Physicochemical and structural properties of meat analogues from yeast and soy protein prepared via high-moisture extrusion. *Food Chemistry, 402*, Article 134265.

Yang, L., Ying, Z., Li, H., Li, J., Zhang, T., Song, Y., & Liu, X. (2023). Extrusion production of textured soybean protein: The effect of energy input on structure and volatile beany flavor substances. *Food Chemistry, 405*, Article 134728.

Yang, S., Zhang, Q., Yang, H., Shi, H., Dong, A., Wang, L., & Yu, S. (2022). Progress in infrared spectroscopy as an efficient tool for predicting protein secondary structure. *International Journal of Biological Macromolecules, 206*, 175–187.

Zhang, J., Liu, L., Liu, H., Yoon, A., Rizvi, S. S., & Wang, Q. (2019). Changes in conformation and quality of vegetable protein during texturization process by extrusion. *Critical Reviews in Food Science and Nutrition, 59*(20), 3267–3280.

Zhang, J., Ying, D., Wei, Y., Zhang, B., Su, X., & Li, S. (2017). Thermal transition and decomposition properties of pH-and phosphate-induced defatted soybean meals. *Journal of Thermal Analysis and Calorimetry, 128*, 699–706.

Zhang, R., Yang, Y., Liu, Q., Xu, L., Bao, H., Ren, X., Jin, Z., & Jiao, A. (2023). Effect of wheat gluten and peanut protein ratio on the moisture distribution and textural quality of high-moisture extruded meat analogs from an extruder response perspective. *Foods, 12*(8), 1696.

Zhang, X., Zhao, Y., Zhang, T., Zhang, Y., Jiang, L., & Sui, X. (2022). High moisture extrusion of soy protein and wheat gluten blend: An underlying mechanism for the formation of fibrous structures. *Lwt, 163*, Article 113561.

Zhang, X., Zhao, Y., Zhang, T., Zhang, Y., Jiang, L., & Sui, X. (2023). Potential of hydrolyzed wheat protein in soy-based meat analogues: Rheological, textural and functional properties. *Food Chemistry: X, 20*, Article 100921.

Zhao, Y.-R., Peng, N., Li, Y.-Q., Liang, Y., Guo, Z.-W., Wang, C.-Y., … Ren, X. (2024). Physicochemical properties, structural characteristics and protein digestibility of pea protein-wheat gluten composited meat analogues prepared via high-moisture extrusion. *Food Hydrocolloids, 156*, Article 110283.

Zhu, H.-G., Tang, H.-Q., Cheng, Y.-Q., Li, Z.-G., & Tong, L.-T. (2021). Potential of preparing meat analogue by functional dry and wet pea (Pisum sativum) protein isolate. *Lwt, 148*, Article 111702.